Effect of Temperature on Elasticity of Clays

SAKURO MURAYAMA, Disaster Prevention Research Institute, Kyoto University

•IN GENERAL, clays behave viscoelastically under external stress and, moreover, such behavior is affected by temperature. There is some type of clay whose stress-strain relation can be expressed by a linear relation with a parameter of time, as long as the applied external stress is less than a certain critical value or the upper yield value. The viscoelastic behavior of the clay skeleton can be analogized with the behavior of the mechanical model. The writer has previously proposed (1) a model that consists of an independent Hookean spring E_1 connected in series with a modified Kelvin element as shown in Figure 1. The latter element is composed of a Hookean spring E_2, a slider σ_2, and a dashpot whose coefficient is obtained from the following equation applying the theory of rate process:

$$\eta = \frac{\sigma_2}{d\epsilon_2/dt} = \frac{\sigma_2}{2A \cdot \sigma_{20} \cdot \sinh(B\sigma_2/\sigma_{20})} \tag{1}$$

where σ_2 is the axial compressive stress distributed on the dashpot, σ_{20} is the magnitude of σ_2 at the initial time when external stress is applied, and ϵ_2 is the axial strain produced in the dashpot. A and B are rheological constants expressed as the following relations:

$$\left.\begin{aligned} A &= A_0 \frac{\varkappa T}{h} \cdot \exp\left(\frac{-E_0}{\varkappa T}\right) \\ B &= \frac{B_0}{T} \end{aligned}\right\} \tag{2}$$

where A_0 and B_0 are constants dependent on soil structure, $\varkappa$ is Boltzmann's constant, h is Planck's constant, T is the absolute temperature of the clay, and E_0 is the free energy of activation. As represented by Eq. 1, this viscosity of clay is a non-Newtonian viscosity or a kind of structural viscosity. This model showed good agreement with the experimental results on undisturbed Osaka marine clay, but further adaptability for other types of clay will be checked in the future.

The influence of temperature on the mechanical behavior of clay has been theoretically explained by several investigators (2, 3), mostly from the point of view of the thermal dependence of the viscosity of clay, but that of the elasticity of clay does not seem to have been thoroughly investigated yet. In these circumstances, the purpose of this study is to investigate the thermal effect on the elasticity of clay, expressed as the independent Hookean spring E_1 and the Hookean spring E_2 in the Kelvin element, by applying the theoretical relations existing under the stress relaxation test.

In the process of mobilizing clay particles, the particles are subjected to the apparent elastic resistance due to the imbalance of the attractive and repulsive physicochemical forces induced by the surrounding particles as well as the viscous resistance due to the adsorbed water interposed between the particles. Therefore, the elasticity of a clay skeleton represented as the spring elements in the mechanical model may be partly due to the flexure of thin plate-like clay particles, but a more effective cause of such elasticity is rather supposed to be due to the physicochemical interparticle force. Moreover, according to the Gouy-Chapman theory, an increase in temperature reduces the double layer thickness and this in turn causes the reduction in the electric repulsion between clay particles (4). Therefore, it may be expected that the elasticity of clay or the elastic constants of the springs in the model can be influenced by temperature.

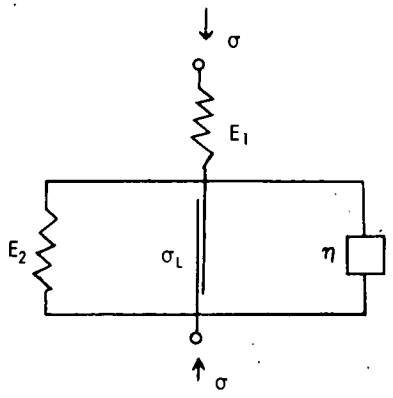

Figure 1. Mechanical model of clay skeleton.

THEORETICAL RELATION UNDER STRESS RELAXATION

The critical compressive stress below which a linear stress-strain relation holds is denoted as the upper yield value σ_u. The model shown in Figure 1 is valid when $\sigma < \sigma_u$. If $B \geq 2$, or

$$B > B\sigma_2/\sigma_{20} \geq 2 \tag{3}$$

the following approximation holds for Eq. 1 within an error of 2 percent:

$$2 \sinh (B\sigma_2/\sigma_{20}) \doteq \exp (B\sigma_2/\sigma_{20}) \tag{4}$$

Therefore the mechanical behavior of the model can be expressed by the following equations:

$$\left.\begin{aligned} \epsilon &= \epsilon_1 + \epsilon_2 \\ \epsilon_1 &= \sigma/E_1 \\ d\epsilon_2/dt &= A \cdot \sigma_{20} \cdot \exp (B\sigma_2/\sigma_{20}) \end{aligned}\right\} \tag{5}$$

where

$$\sigma_2 = \sigma - \sigma_\ell - E_2 \epsilon_2, \quad \sigma_{20} = \sigma - \sigma_\ell$$

The relaxation of stress in a clay skeleton under a constant axial initial strain ϵ_0 can be analyzed through solution of Eq. 5 under the following condition:

$$\epsilon = \epsilon_1 + \epsilon_2 = \epsilon_0 \tag{6}$$

Since ϵ_2 is zero at t = 0, stress in a clay skeleton at t = 0 is obtained as

$$\sigma_{t=0} = E_1 \epsilon_0 \tag{7}$$

Substituting the second equation of Eq. 5 and Eq. 6 into the fourth equation of Eq. 5 σ_2 becomes

$$\sigma_2 = [(E_1 + E_2)\sigma - E_1\sigma_\ell - E_1E_2\epsilon_0]/E_1 \tag{8}$$

Similarly, from Eqs. 5 and 7, σ_{20} becomes

$$\sigma_{20} = E_1\epsilon_0 - \sigma_\ell \tag{9}$$

By substitution of Eqs. 8 and 9 into Eq. 3, the validity condition for σ is transformed as

$$\epsilon_0 E_1 > \sigma \geq \frac{E_1E_2}{E_1 + E_2}\left[\epsilon_0\left(1 + \frac{2E_1}{BE_2}\right) + \frac{\sigma_\ell}{E_2}\left(1 - \frac{2}{B}\right)\right] \tag{10}$$

The fundamental equation of stress relaxation is obtained by eliminating ϵ_2 from the third equation of Eq. 5 as follows, provided that B is large and exp (– B) is negligibly small:

$$\left.\begin{aligned} \sigma &= \frac{E_1E_2}{E_1 + E_2}\left[\left(\epsilon_0 + \frac{\sigma_\ell}{E_2}\right) - \left(\epsilon_0 - \frac{\sigma_\ell}{E_1}\right)\frac{E_1}{BE_2}\log (Rt)\right] \\ R &= A \cdot B \cdot (E_1 + E_2) \end{aligned}\right\} \tag{11}$$

where

If σ is beyond the limit expressed by Eq. 10 and at $t \to \infty$, σ is obtained by substituting $\sigma_2 = 0$ into Eq. 8 as follows:

$$\sigma_{t \to \infty} = \frac{E_1 E_2}{E_1 + E_2} \left(\epsilon_0 + \frac{\sigma_\ell}{E_2} \right) \tag{12}$$

It is shown from Eqs. 11 and 12 that the stress σ decreases linearly with the logarithm of time until σ reaches the limiting value expressed by Eq. 10 and finally it relaxes to a finite value of $\sigma_{t \to \infty}$. Because this relation is valid only when $\sigma \leq \sigma_u$, the critical initial strain ϵ_{oc} beyond which the instantaneous axial stress exceeds σ_u is given by

$$\epsilon_{oc} = \sigma_u / E_1 \tag{13}$$

Eliminating ϵ_0 from Eqs. 7 and 12, we obtain

$$E_2 = \frac{\sigma_{t \to \infty} - \sigma_\ell}{\sigma_{t=0} - \sigma_{t \to \infty}} \cdot E_1 \equiv \alpha \cdot E_1 \tag{14}$$

By differentiation of Eq. 11, we obtain

$$-\frac{d\sigma}{d \log t} = \frac{E_1^2}{B(E_1 + E_2)} \left(\epsilon_0 - \frac{\sigma_\ell}{E_1} \right) \tag{15}$$

Substituting Eqs. 2, 7, and 14 into Eq. 15, we obtain

$$-\frac{d\sigma}{d \log t} = \frac{\sigma_{t=0} - \sigma_{t \to \infty}}{B_0} \cdot T = \frac{\sigma_{t \to \infty} - \sigma_\ell}{\alpha \cdot B_0} \cdot T \tag{16}$$

If a certain temperature T_a deg K is adopted as a standard, Eq. 16 is transformed as

$$\left.\begin{aligned} \sigma_{t \to \infty} &= \frac{k \cdot \alpha \cdot B_0}{T_a} \left(-\frac{d\sigma}{d \log t} \right) + \sigma_\ell \\ \text{where} \quad k &= T_a / T \,, \quad \alpha = E_2 / E_1 \end{aligned}\right\} \tag{17}$$

From Eq. 14, $\sigma_{t \to \infty}$ is given by

$$\sigma_{t \to \infty} = \frac{\alpha}{1 + \alpha} \sigma_{t=0} + \frac{1}{1 + \alpha} \sigma_\ell \tag{18}$$

When the second term $\sigma_\ell / (1 + \alpha)$ of the right-hand side of Eq. 18 is negligibly small compared with the term of the left-hand side, Eq. 18 can be written approximately as

$$\sigma_{t \to \infty} = \frac{\alpha}{1 + \alpha} \sigma_{t=0} \tag{19}$$

STRESS RELAXATION TESTS UNDER UNIAXIAL STRAIN

The specimens used for stress relaxation tests were of undisturbed clay obtained from the Osaka diluvial layer. The results of physical tests of the clay are as follows: specific gravity, 2.57; L. L., 76.2 percent; P. L., 30.7 percent; contents of clay, silt, and sand, 45, 38, and 17 percent respectively.

The maximum preconsolidation stress measured by oedometer tests is 3.8 kg/cm^2. The lower yield value σ_ℓ measured by flow tests is 0.01 kg/cm^2. The upper yield value σ_u is determined as the stress corresponding to the first inflection point of the stress-

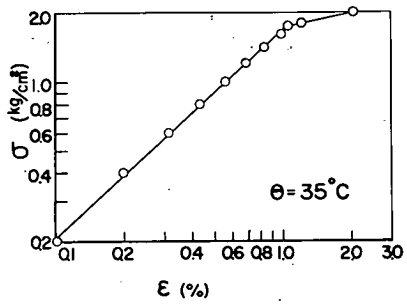

Figure 2. Logarithmic relation of stress vs strain in stress-controlled compression test to determine upper yield value.

strain curve on logarithmic paper, which is obtained by a stress-controlled undrained test whose load is added in equal increments at uniform time intervals. By this procedure σ_u is determined as 1.75 kg/cm^2 at 35 C, as shown in Figure 2. The cylindrical clay specimen (height 8.0 cm, diameter 3.57 cm) was covered by a thin rubber membrane and was placed in a triaxial compression cell of a plastometer. This plastometer (2) consists of a triaxial compression testing unit and a recording and controlling unit. In the case of the stress relaxation test, a constant axial deformation applied on the specimen can be read on the scale indicator of the plastometer and its response in the axial stress is automatically and continuously recorded by the recording unit. In the cell of the testing unit, water of definite temperature but of no pressure was circulated to keep the specimen at constant temperature. After the temperature of the specimen reached the equilibrium state, constant axial strain ϵ_0 was instantaneously applied on the specimen under undrained condition, then the axial stress σ was recorded electronically with the time by the plastometer.

Examples of the results of the stress relaxation tests at 30 C for various initial strains (ϵ_0 = 0.25, 0.5, 0.75, 1.00, 1.50, and 2.00 percent) reproduced from the recrods are shown in Figure 3. This figure shows that the axial stress σ decreases proportionately with the logarithm of time for some period and finally approaches a finite value $\sigma_{t\to\infty}$ as predicted by Eqs. 11 and 12. Therefore from the record of the plastometer

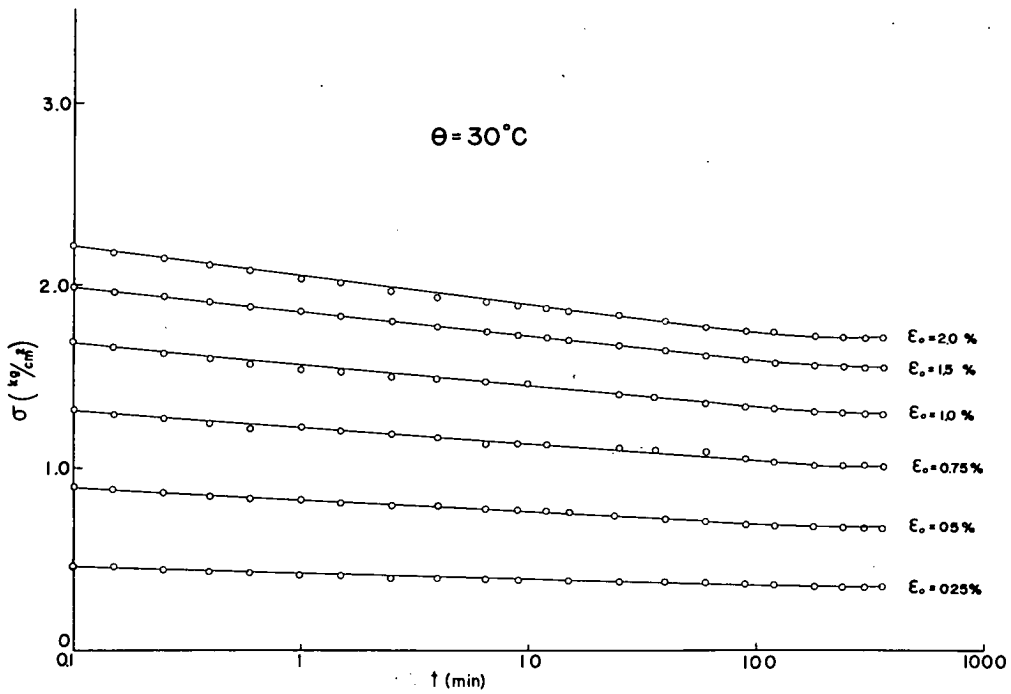

Figure 3. Curves representing axial stress vs elapsed time relation during stress relaxation.

the initial axial stress $\sigma_t = 0$ caused by the instantaneously applied strain can be read and from Figure 3 the rate of stress relaxation $d\sigma/d\log t$ and the final axial stress $\sigma_{t\to\infty}$ can be measured for each applied initial strain ϵ_0 and each temperature θ C.

EXPERIMENTAL RESULTS

The similar stress relaxation tests indicated in Figure 3 were performed under various temperatures, namely θ = 10, 20, and 40 C. From these tests, values of $\sigma_t = 0$, $\sigma_{t\to\infty}$, and $d\sigma/d\log t$ were observed in the various cases of ϵ_0 and θ. The following consideration will be developed on the basis of these values.

If the standard temperature T_a ($T_a = 273 + \theta_a$) defined in Eq. 17 is adopted as 313 (θ_a = 40 C, T_a = 273 + 40 = 313), the value of K in Eq. 17 is given by

$$K = \frac{T_a}{T} = \frac{313}{\theta + 273}$$

According to the theoretical consideration, the relation between $d\sigma/d\log t$ and $\sigma_{t\to\infty}$ and that between $\sigma_{t=0}$ and $\sigma_{t\to\infty}$ can be represented by Eqs. 17 and 19, as long as the applied initial strain ϵ_0 is less than the critical strain expressed by Eq. 13. Therefore if observed values of $K\left(-\frac{d\sigma}{d\log t}\right)$ and $\sigma_t = 0$ are plotted against $\sigma_{t\to\infty}$ on a natural scale, these relationships are expected to be represented by straight lines extending to a certain limit. Figure 4 shows these relationships obtained by plotting all the observed values. Since the plotted points within a certain limit will lie along two straight lines starting from the vicinities of the origin of axes as predicted by Eqs. 17 and 19, the experimental relations can be expressed by the following linear equations independent of temperature:

$$\left.\begin{aligned} \sigma_{t\to\infty} &= (2/3)\cdot\ \sigma_t = 0 \\ \sigma_{t\to\infty} - \sigma_\ell &\doteqdot 9.5\left[K\left(-\frac{d\sigma}{d\log t}\right)\right] \\ \sigma_\ell &\doteqdot 0.01\ \mathrm{kg/cm^2} \end{aligned}\right\} \qquad (20)$$

Referring the first equation in Eq. 20 to Eq. 19, α is given by

$$\alpha \doteqdot 2 \quad (\text{where } \alpha = E_2/E_1) \qquad (21)$$

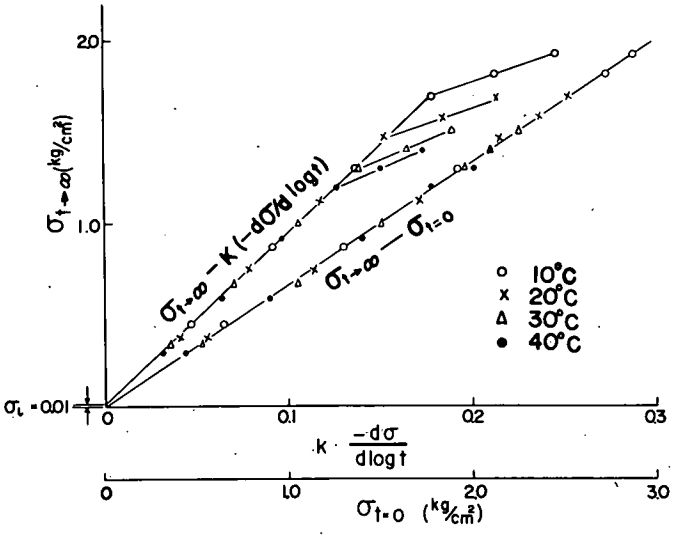

Figure 4. Relationship among $K\cdot(-d\sigma/d\log t)$, $\sigma_{t=0}$ and $\sigma_{t\to\infty}$ under various temperatures.

This relation shows that the values of elastic moduli E_1, E_2 are proportional to each other irrespective of temperature. Moreover, in Figure 4. the experimental relationship between t = 0 and $\sigma_{t\to\infty}$ is represented by a straight line for whole value of $\sigma_{t=0}$. From this result, therefore, the linear relation between E_1 and E_2 seems to be still valid even if ϵ_0 exceeds the critical strain ϵ_{oc}.

While the linear relationship between $K(-d\sigma/d \log t)$ and $\sigma_{t\to\infty}$ is valid only within a certain limit of the straight line as shown in Figure 4, in the region beyond this limit the relationship deviates from this straight line and is represented by a short, gently inclined line. Therefore the relation between $d\sigma/d \log t$ and $\sigma_{t\to\infty}$ seems to be affected by the applied initial strain ϵ_0

In order to investigate the effects of ϵ_0 on the values of $\sigma_{t=0}$, $\sigma_{t\to\infty}$, and $d\sigma/d \log t$, these experimental values are plotted against ϵ_0 as shown in Figures 5, 6, and 7. These figures show that these relationships are linear within the same strain range up to about 0.95 percent of ϵ_0, where they deflect to become a gentler gradient. Since the strain corresponding to the deflection point should be the critical initial strain ϵ_{oc}, it can be said that the value of ϵ_{oc} is kept constant independent of temperature.

In order to observe the influence of temperature on $\sigma_{t=0}$, $\sigma_{t\to\infty}$, and $d\sigma/d \log t$, Figures 5, 6, and 7 are rearranged as shown in Figures 8, 9, and 10, respectively.

From each set of $\sigma_{t=0}$ lines in Figure 5 and $\sigma_{t\to\infty}$ lines in Figure 6 corresponding to the same temperature, the elastic moduli E_1 and E_2 at this temperature can be computed through Eqs. 7, 19, and 21. In Figure 11 the elastic moduli thus computed are plotted against ϵ_0. From these figures, it is observed that E_1 and E_2 at a certain temperature are kept constant within the limit of ϵ_{oc}, but beyond this limit they decrease with the increase of ϵ_0. This suggests that the fracture in the clay skeleton proceeds with the applied strain exceeding the value of ϵ_{oc}. The effect of temperature on the elastic moduli is shown in Figure 12, in which the constant elastic moduli shown in Figure 11 are plotted against their respective temperatures. From these figures it can be concluded that the elasticity of clay decreases with the increase in temperature.

As stated, the value of ϵ_{oc} is kept constant independent of temperature and E_1 at a certain temperature is also kept constant as long as ϵ_0 is less than ϵ_{oc}, and therefore the value of E_1 at a certain temperature can be calculated by the data shown in Figure 2. In Figure 2, since the upper yield value of this clay is 1.75 kg/cm^2 at 35 C, the value of E_1 at this temperature

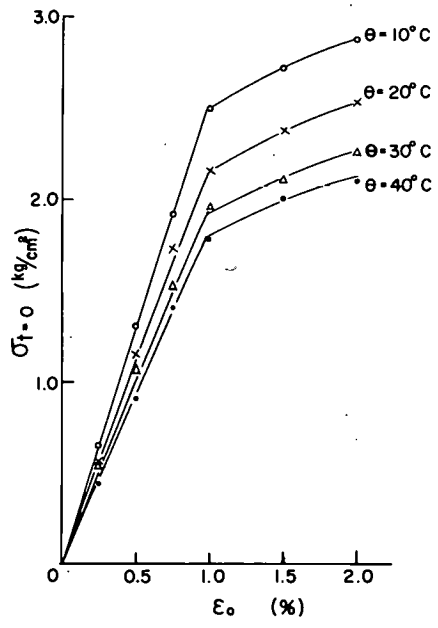

Figure 5. Relationship between initial axial stress $\sigma_{t=0}$ and initially applied axial strain ϵ_0.

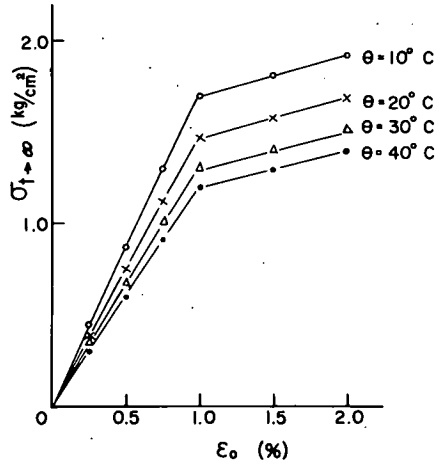

Figure 6. Relationship between final axial stress $\sigma_{t\to\infty}$ and initially applied axial strain ϵ_0.

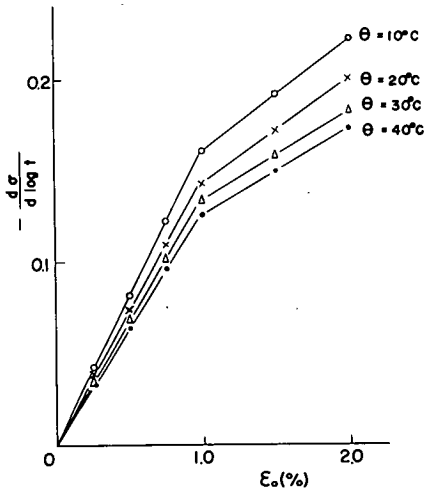

Figure 7. Relationship between rate of stress relaxation $d\sigma/d \log t$ and initially applied axial strain ϵ_0.

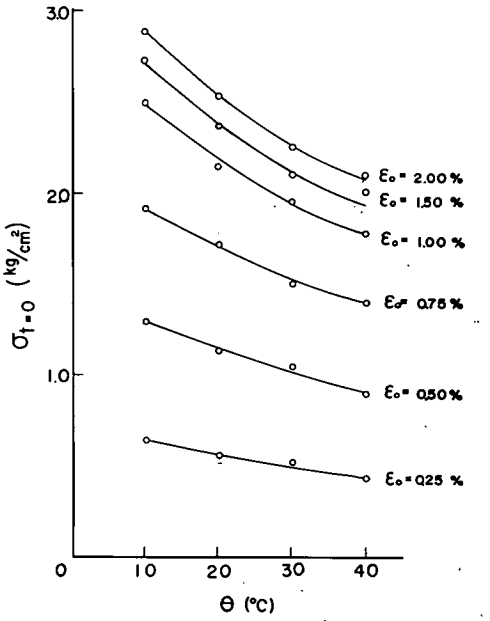

Figure 8. Relationship between initial axial stress $\sigma_{t=0}$ and temperature θ.

can be calculated by Eq. 13:

$$E_1 = \sigma_u/\epsilon_{oc} \doteq 1.75/0.0095 = 185 \text{ kg/cm}^2 \tag{22}$$

Referring the theoretical equation of Eq. 17 to the experimental relations of Eq. 21 and the second equation of Eq. 20, a rheological constant B_0 can be obtained as follows:

$$B_0 = \frac{9.5 \cdot T_a}{\alpha} = \frac{9.5}{2} T_a = 4.75\ T_a \tag{23}$$

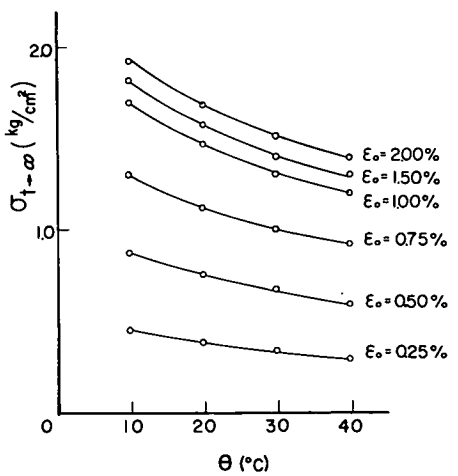

Figure 9. Relationship between final axial stress $\sigma_{t\to\infty}$ and temperature θ.

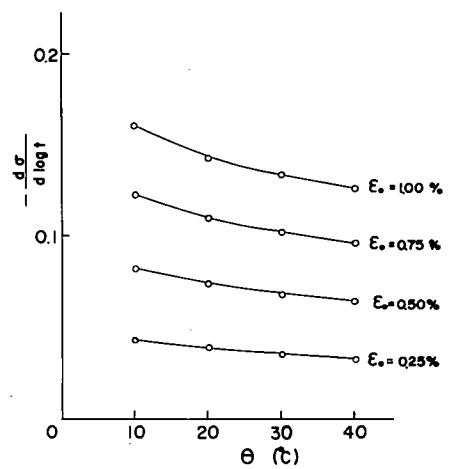

Figure 10. Relationship between rate of stress relaxation $d\sigma/d \log t$ and temperature θ.

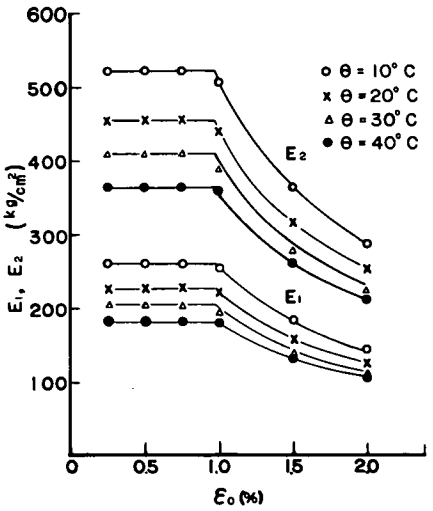

Figure 11. Elastic moduli related to initially applied strain under various temperatures.

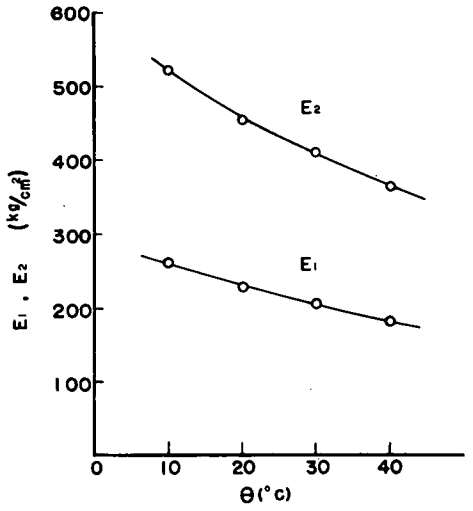

Figure 12. Relationship between elastic moduli of the mechanical model shown in Figure 1 and temperature.

Hence B is expressed as

$$B = B_0/T = 4.75 \cdot 313/(\theta + 273) \tag{24}$$

Computed values of B from Eq. 23 for θ = 10, 20, 30, and 40 C are 5.25, 5.07, 4.90, and 4.75 respectively. This relation is represented by a curve in Figure 13.

RELATION BETWEEN THE RESULTS OF STRESS RELAXATION TESTS AND FLOW TESTS

Solving Eq. 5 under the condition of σ = constant, the equation for normal flow is obtained as

$$\epsilon = \frac{\sigma}{E_1} + \frac{\sigma - \sigma_l}{E_2} + \frac{\sigma - \sigma_l}{BE_2} \log(A \cdot B \cdot E_2 \cdot t) \tag{25}$$

By the differentiation, we get

$$\frac{1}{BE_2} = \frac{d\epsilon}{d \log t} \cdot \frac{1}{\sigma - \sigma_l} \tag{26}$$

The uniaxial compression flow tests under undrained conditions were performed on the same clay sample used on the stress relaxation tests. Figure 14 is the relationship between $d\epsilon/d \log t$ and applied stress σ obtained by the flow tests at 20 C. From this figure, the lower yield value σ_l is read ad 0.01 kg/cm^2. Figure 15 shows curves representing the flow strain ϵ against time t relation obtained by the flow test of σ = 1 kg/cm^2 under various temperatures (θ = 10, 20, 30, and 40 C). Applying the value of $d\epsilon/d \log t$ in Figure 15 to Eq. 26, BE_2 can be computed.

In the flow test shown in Figure 15, the initial axial strain $\epsilon_{t=0}$ when the load is applied was also observed for each temperature condition. Measured values of $\epsilon_{t=0}$ for θ = 10, 20, 30, and 40 C were 0.393, 0.419, 0.623, and 0.705 percent, respectively. Applying these initial strains to Eq. 7, values of E_1 are obtained. Besides, since Eq. 21 may also be valid for this clay under the flow testing, E_2 can be obtained by multiplying the E_1 obtained above by α. From the values of BE_2 and E_2, B can be computed

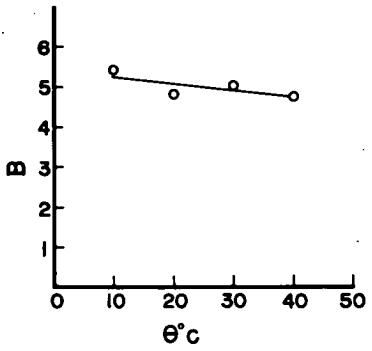

Figure 13. Relationship of rheological constant B vs temperature θ.

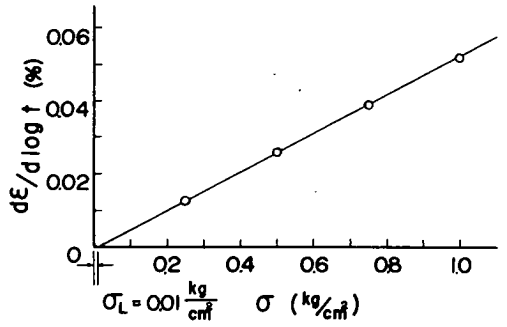

Figure 14. Relationship between rate of flow strain dε/d logt t and applied σ obtained by flow tests (20 C).

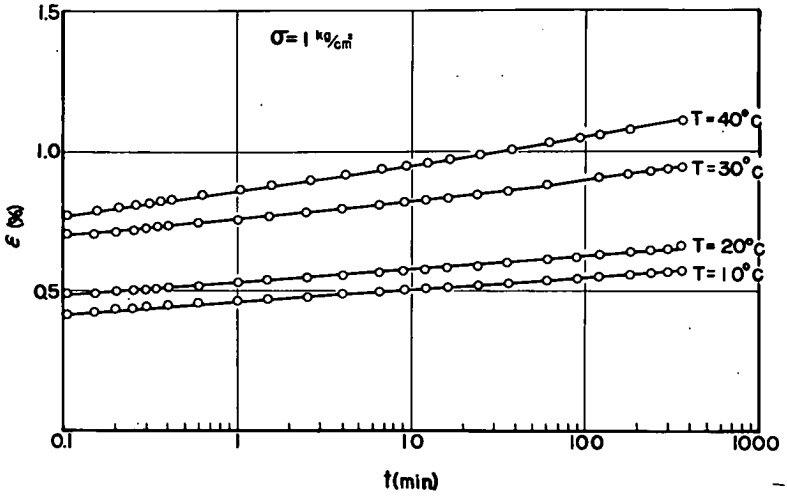

Figure 15. Curves representing axial strain ε vs time t relation during flow under various temperatures.

for each temperature condition, and the computed values of B are plotted in Figure 13 as points. In the figure, these points do not lie well on the line obtained by the stress relaxation tests. But this discrepancy may be supposed to be due mainly to the heterogeneity of the undisturbed diluvial clay sample.

CONCLUSIONS

Because clay is a viscoelastic material, it is necessary to investigate its mechanical behavior from the point of view of its elasticity as well as its viscosity. The mechanical behavior of the clay skeleton whose stress and strain are expressed by a linear relation with a parameter of time has been simulated by the model shown in Figure 1. The viscosity of clay is influenced by temperature as suggested in the flow behavior at various temperatures. Similarly, the effect of temperature on the elasticity of clay can be investigated by the behavior on the stress relaxation tests at various temperatures. In this study the effect of temperature on the elastic moduli in the model is investigated. The main results obtained are as follows:

1. The behavior of Osaka marine clay under the stress relaxation test is well predicted by the mechanical model proposed by the writer.

2. As the value of the rheological constant B obtained by flow tests practically concides with that obtained by stress relaxation tests, the equations of Eq. 5 are verified to express the behaviors in both testing procedures, irrespective of temperature.

3. Elastic moduli E_1 and E_2 are kept constant within the limit of a critical initial strain ϵ_{oc}, but beyond this limit they decrease with the increase of initial strain. The latter behavior suggests the occurrence of a fracture in a clay skeleton

4. The critical initial strain ϵ_{oc} is kept constant independent of temperature.

5. Ratio of E_1 to E_2 is constant independent of temperature and also seems to be constant independent of the magnitude of applied initial strain ϵ_0.

6. Elastic moduli E_1 and E_2 measured within the limit of ϵ_{oc} decrease with the increase in temperature.

ACKNOWLEDGMENT

The writer wishes to express his deep appreciation to Mr. Kunio Iida for his sincere cooperation in these experimental studies.

REFERENCES

1. Murayama, S., and Shibata, T. On the Rheological Characters of Clay, Part I. Bulletin No. 26, Disaster Prevention Research Inst., Kyoto Univ., 1958.
   Murayama, S., and Shibata, T. Flow and Stress Relaxation of Clays. Proc. Rheology and Soil Mech. Symposium of IUTAM, Grenoble, France, April 1964, p. 99-129.
2. Murayama, S., and Shibata, T. Rheological Properties of Clays. Proc. Fifth Internat. Conf. on Soil Mech. and Found. Eng., Paris, 1961, p. I-269-273.
3. Mitchell, J. K., Campanella, R. G., and Singh, A. Soil Creep as a Rate Process. Jour. Soil Mech. and Found. Div., ASCE, Vol. 94, No. SM1, Proc. Paper 5751, Jan. 1968, p. 231-253.
4. Lambe, T. W. The Structure of Compacted Clay. Jour. Soil Mech. and Found. Div. ASCE, Vol. 84, No. SM2, Proc. Paper 1954, May 1958, p. 1654-7.